Supplementary Information

ALK5-dependent TGF-β signaling is a major determinant of late stage adult neurogenesis

Yingbo He, Hui Zhang, Andrea Yung, Saul A Villeda, Philipp A Jaeger, Oluwatobi Olayiwola, Nina Fainberg, and Tony Wyss-Coray

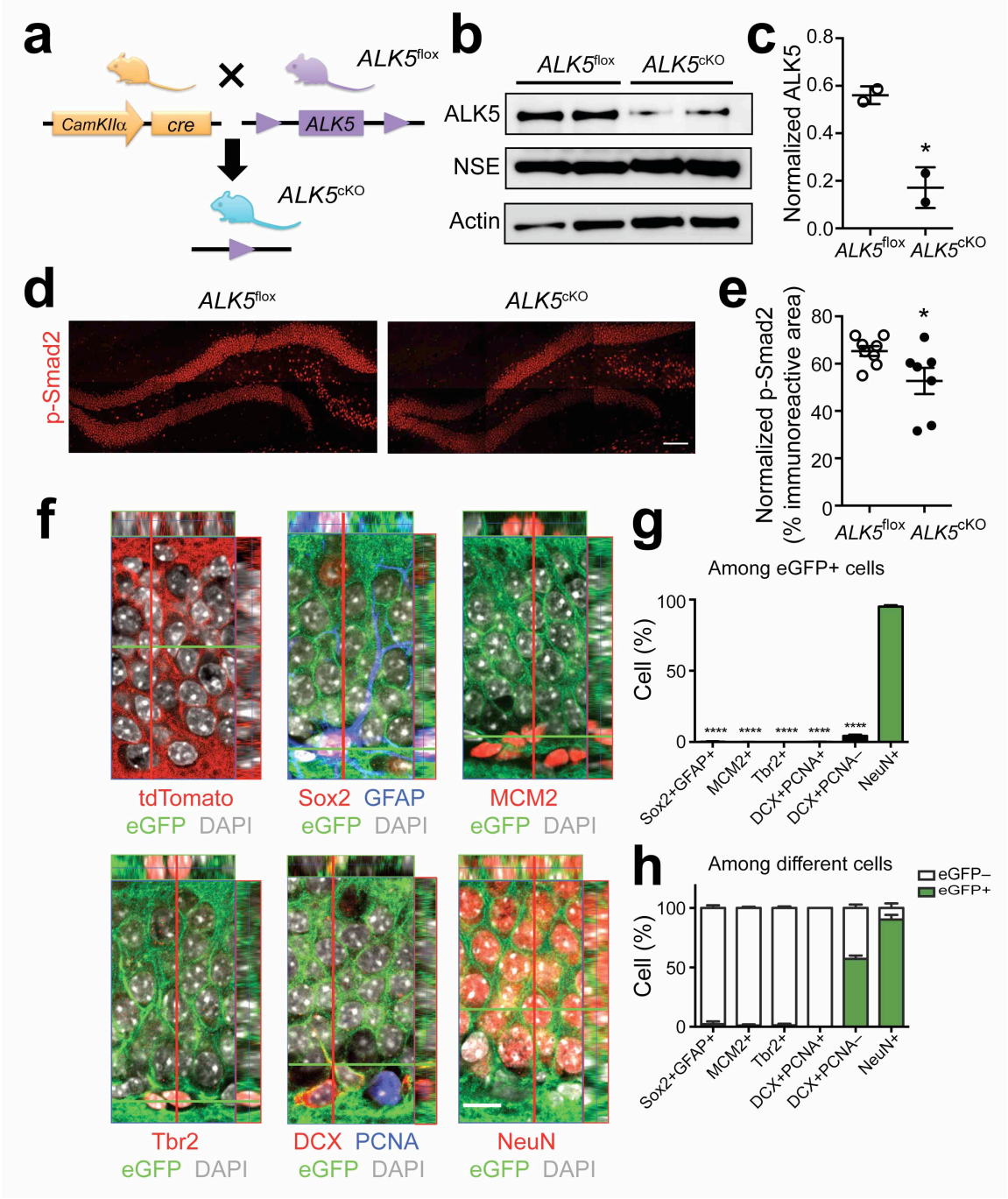

Supplementary Figure 1. Construction and characterization of *ALK5*^{cKO} transgenic mice. (a) Diagram of gene constructs used to create *ALK5*^{cKO} mice. (b,c) Immunoblot of hippocampal lysates from 3-month-old *ALK5*^{flox} and *ALK5*^{cKO} mice probed with antibodies against ALK5, NSE, and actin in (b) and quantification of ALK5 signal intensity normalized against NSE in (c), n = 2 mice per group, P = 0.0276. Full-length blots are presented in Supplementary Figure 10. The experiments were independently performed twice. (d,e) Representative tiled confocal images (d) and quantification (e) of the dentate gyrus from 3-month-old *ALK5*^{flox} (n = 8) and *ALK5*^{cKO} (n = 7) mice immunostained for p-Smad2. P-Smad2 signals were normalized to background in (e). Three sections per

mouse, P = 0.0433. (f) Representative orthogonal projections from confocal Z-stack images of the dentate gyrus from 3-month-old *mT/mG* mice before and after crossing with *CamKIIα-cre* mice immunostained for eGFP in combination with Sox2 plus GFAP, MCM2, Tbr2, DCX plus PCNA, and NeuN. DAPI stains nuclei. Scale bar is 100 μm in (d) and 10 μm in (f). (g) Quantification of eGFP positive cells in different cell types detected in (f) from the dentate gyrus. (h) Quantification of eGFP positive and negative cells in individual cell types detected in (f) from the dentate gyrus. n = 4 mice, 3 sections per mouse in (g,h). Data are presented as mean ± s.d. in (c), mean ± s.e.m. in (e,g,h). *P < 0.05, ****P < 0.0001 Student's t-test in (c,e); one-way ANOVA, Dunnett's post-hoc test in (g).

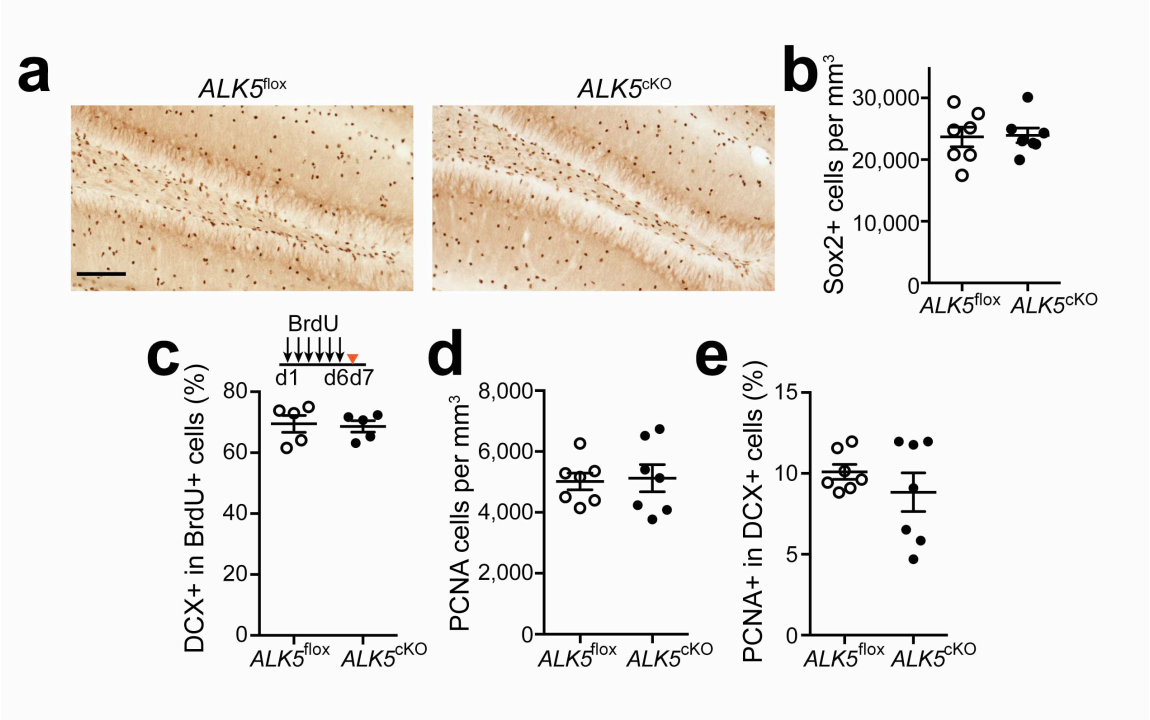

Supplementary Figure 2. Deficiency of ALK5 is not affecting the neural stem cell pool and production of committed neurons. (a,b) Immunohistochemical detection (a) and quantification (b) of Sox2 labeled cells in the dentate gyrus of 3-month-old *ALK5*^{flox} and *ALK5*^{cKO} mice (n = 7 mice per group, 5 sections per mouse, *P* = 0.9023). (c) Quantification of the percentage of BrdU and DCX double-labeled cells in the dentate gyrus from 7-month-old *ALK5*^{flox} and *ALK5*^{cKO} mice after short-term BrdU labeling (n = 5 mice per group, 5 sections per mouse, *P* = 0.8043). Experimental design inserted on top. (d) Quantification of total PCNA+ proliferating cells in the dentate gyrus of 3-month-old *ALK5*^{flox} and *ALK5*^{cKO} mice (n = 7 mice per group, 5 sections per mouse, *P* = 0.8384) (e) Quantification of the percentage of DCX and PCNA double-labeled cells in the dentate gyrus of 3-month-old *ALK5*^{flox} and *ALK5*^{cKO} mice (n = 7 mice per group, 5 sections per mouse, *P* = 0.3450). Scale bar is 100 μm. Data are presented as mean ± s.e.m. Student's t-test.

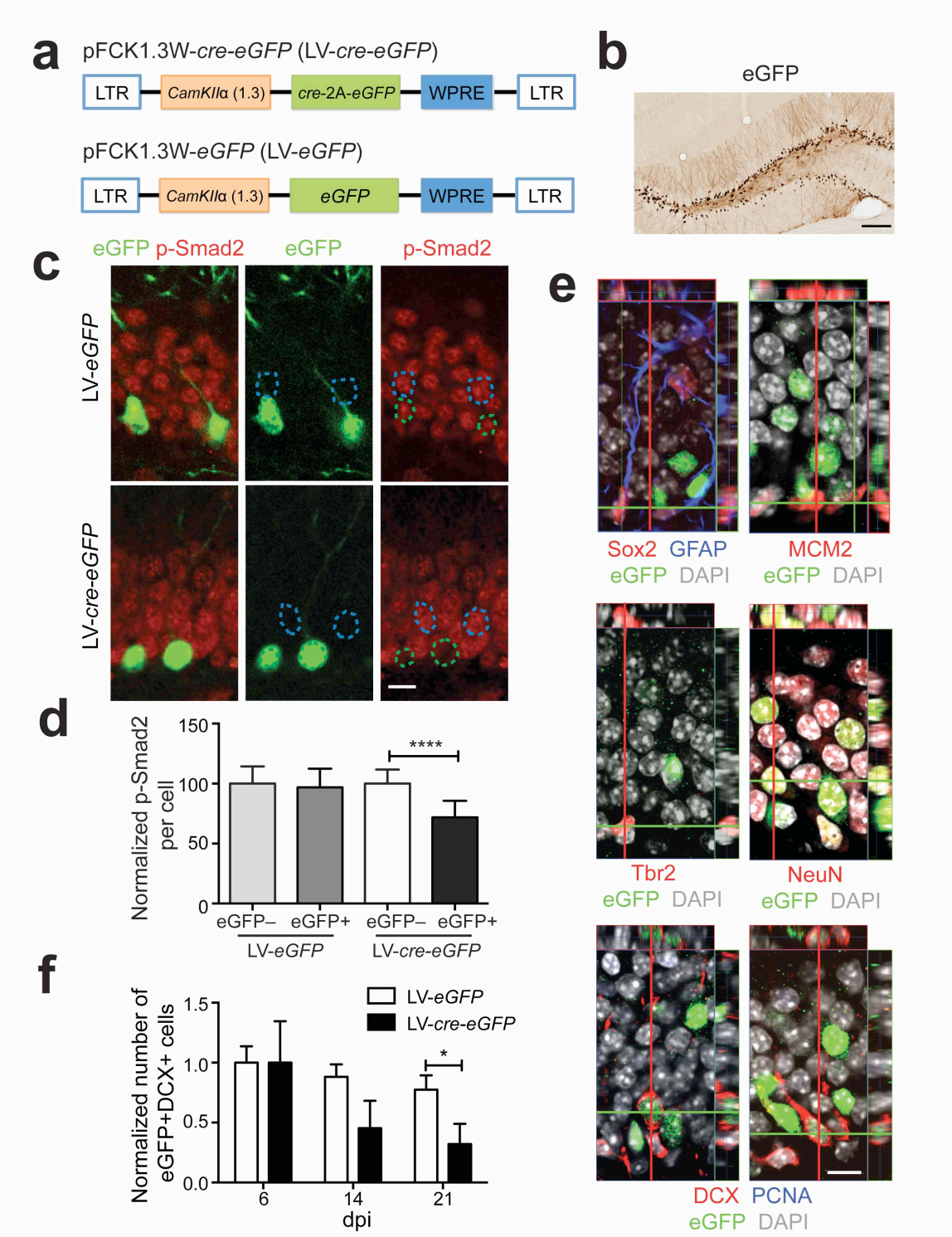

Supplementary Figure 3. Construction and characterization of cre lentivirus that decreases the survival of infected newborn neurons in *ALK5*^{flox} mouse dentate gyrus. (a) Design of the lentiviral vectors. (b) Immunohistochemical detection of eGFP labeled lentivirus-infected cells in the dentate gyrus of stereotaxically injected 2-month-old *ALK5*^{flox} mice. (c,d) Representative confocal images (c) and quantification (d) of lentivirus-injected dentate gyrus from 3-month-old *ALK5*^{flox} mice immunostained for p-

Smad2 and eGFP. P-Smad2 signals were normalized to signals in uninfected cells in (d). Green or blue dashed circles highlight the cell bodies of eGFP+ or eGFP– neurons. n = 27, 21, 24, 23 neurons from three mice total for eGFP–/LV-*eGFP*, eGFP+/LV-*eGFP*, eGFP–/LV-*cre-eGFP*, eGFP+/LV-*cre-eGFP* group, respectively. (e) Representative orthogonal projections from confocal Z-stack images of LV-*cre-eGFP* lentivirus-injected dentate gyrus of 2-month-old *ALK5*^{flox} mice immunostained for eGFP in combination with Sox2 plus GFAP, MCM2, Tbr2, DCX plus PCNA, and NeuN. DAPI stains nuclei. Scale bar is 100 μm in (b) and 10 μm in (c,e). (f) Quantification of the number of lentivirus-infected eGFP and DCX double-labeled newborn neurons in the dentate gyrus from LV-*cre-eGFP* and LV-*eGFP* stereotaxically injected *ALK5*^{flox} mice with 2 months of age at 6, 14, and 21 dpi. Cell numbers were normalized to values at 6 dpi. n = 4 mice per group, 4 sections per mouse. **P* = 0.0355. Data are presented as mean + s.d. in (d) and mean + s.e.m. in (f). *****P* < 0.0001. One-way ANOVA, Tukey's post-hoc test (d); one-tailed Student's t-test (f).

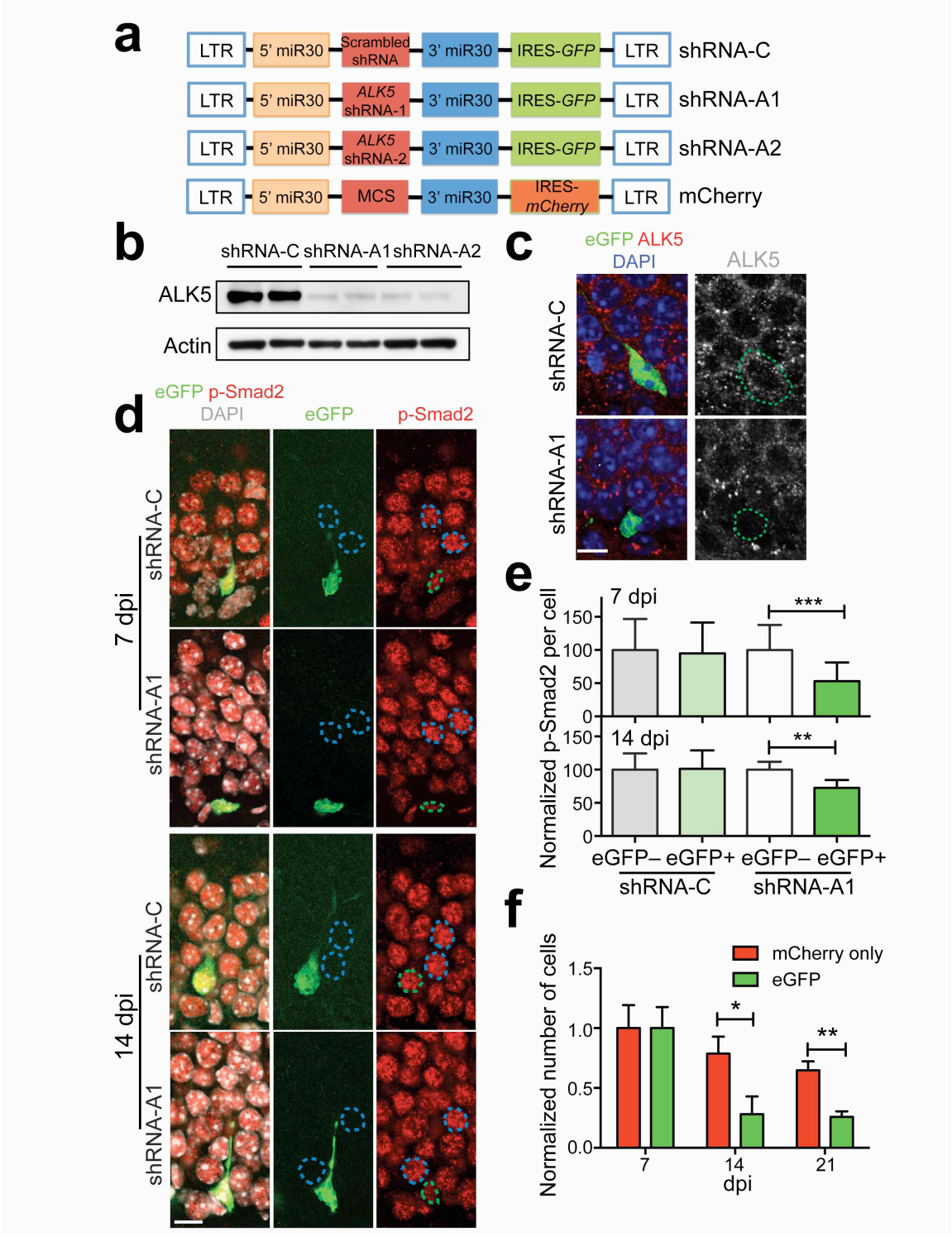

Supplementary Figure 4. Construction and characterization of *ALK5* shRNA retroviruses that decrease the survival of infected newborn neurons in C57BL/6 mouse dentate gyrus. (a) Design of the retroviral vectors. MCS, multiple cloning site. (b) Immunoblot of lysates from HEK293T cells co-transfected with an expression vector for *ALK5* and different shRNAs probed with antibodies against ALK5 and actin. Full-length blots are presented in Supplementary Figure 10. (c,d) Representative confocal images

of retrovirus-injected dentate gyrus of 2-month-old C57BL/6 mice immunostained for eGFP and ALK5 at 7 dpi in (c) or eGFP and p-Smad2 at both 7 dpi and 14 dpi in (d). DAPI stains nuclei. Green or blue dashed circles highlight the cell bodies of eGFP+ or eGFP– neurons. Scale bar is 10 μm. (e) Quantification of p-Smad2 signal intensity from (d). P-Smad2 signals were normalized to signals in uninfected cells in (e). n = 20, 20, 23, 23 neurons from four mice total for eGFP–/shRNA-C, eGFP+/shRNA-C, eGFP–/shRNA-A1, eGFP+/shRNA-A1 group at 7 dpi, respectively. n = 15, 15, 14, 14 neurons from four mice total for eGFP–/shRNA-C, eGFP+/shRNA-C, eGFP–/shRNA-A1, eGFP+/shRNA-A1 group at 14 dpi, respectively. (f) Quantification of the number of virus-infected mCherry only and eGFP-labeled (eGFP only and eGFP/mCherry double-labeled) newborn neurons in the dentate gyrus from stereotaxically injected 2-month-old female C57BL/6 mice at 7 (n = 5 mice), 14 (n = 4 mice, $P = 0.0485$), and 21 dpi (n = 5 mice, $P = 0.0021$). Four sections per mouse. Cell numbers were normalized to values at 7 dpi. Data are presented as mean + s.d. in (e) and mean + s.e.m. in (f). *$P < 0.05$, **$P < 0.01$, ***$P < 0.001$. One-way ANOVA, Tukey's post-hoc test (e); Student’s t-test (f).

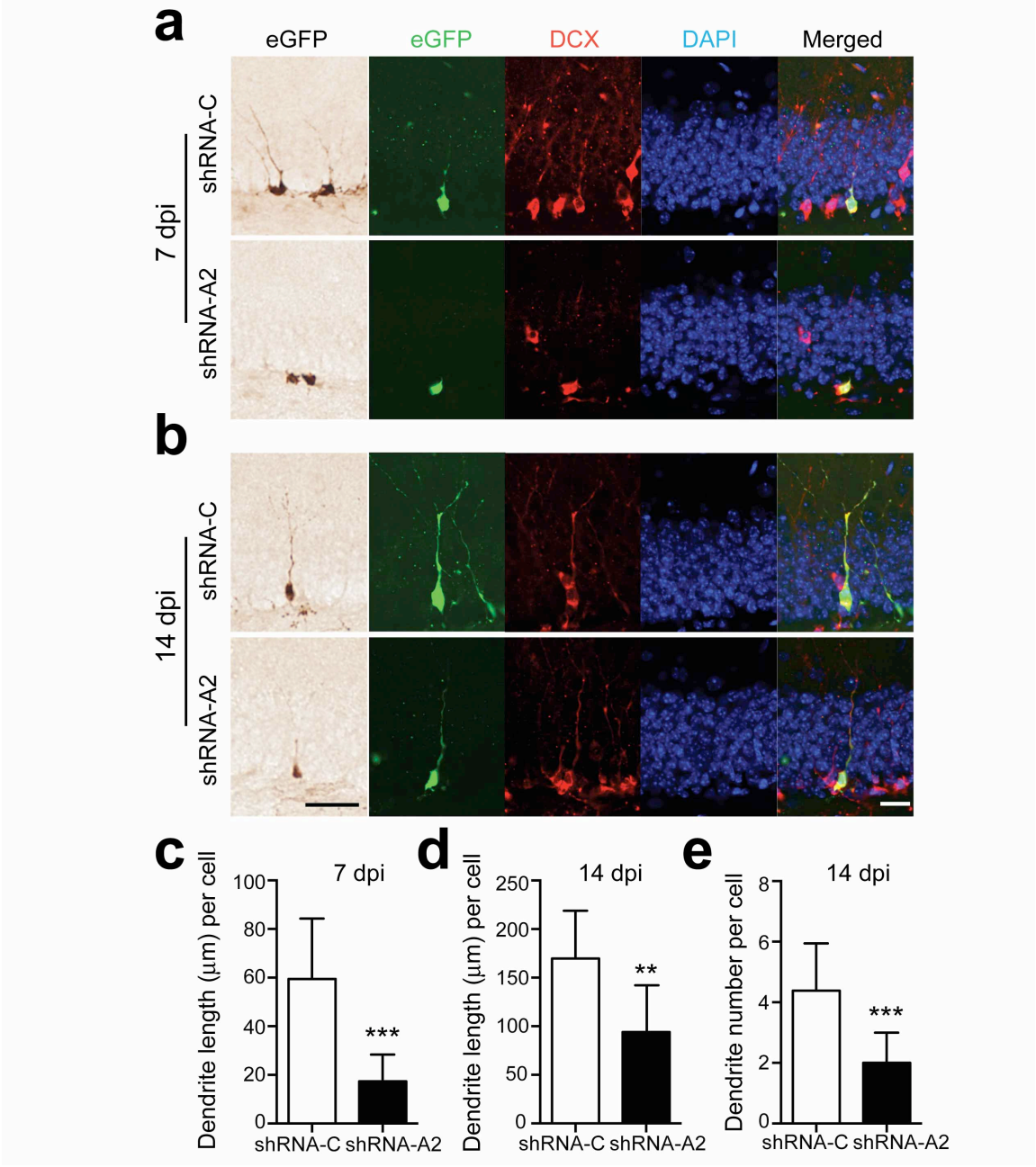

Supplementary Figure 5. Knockdown of ALK5 by shRNA-A2 retrovirus in progenitor cells decelerates dendrite development of newborn neurons in the dentate gyrus. (a,b) Brightfield immunohistochemical detection of virus-infected eGFP-immunostained cells (left) and confocal images of eGFP, DCX, and DAPI triple-labeled newborn neurons (right) in the dentate gyrus of stereotaxically injected 2-month-old C57BL/6 mice at 7 (a) and 14 dpi (b). Scale bar is 50 µm in brightfield immunohistochemical images and 20 µm in confocal images. (c) Quantification of dendritic length of virus-infected newborn neurons in the dentate gyrus at 7 dpi. (d,e) Quantification of dendritic length (d) and number (e) of virus-infected newborn neurons in the dentate gyrus at 14 dpi. n = 17, 12 neurons from two mice total for each group at 7 dpi. n = 13, 9 neurons from two mice total for each group at 14 dpi. Data are presented as mean + s.d. $^{**}P < 0.01$, $^{***}P < 0.001$, Student's t-test.

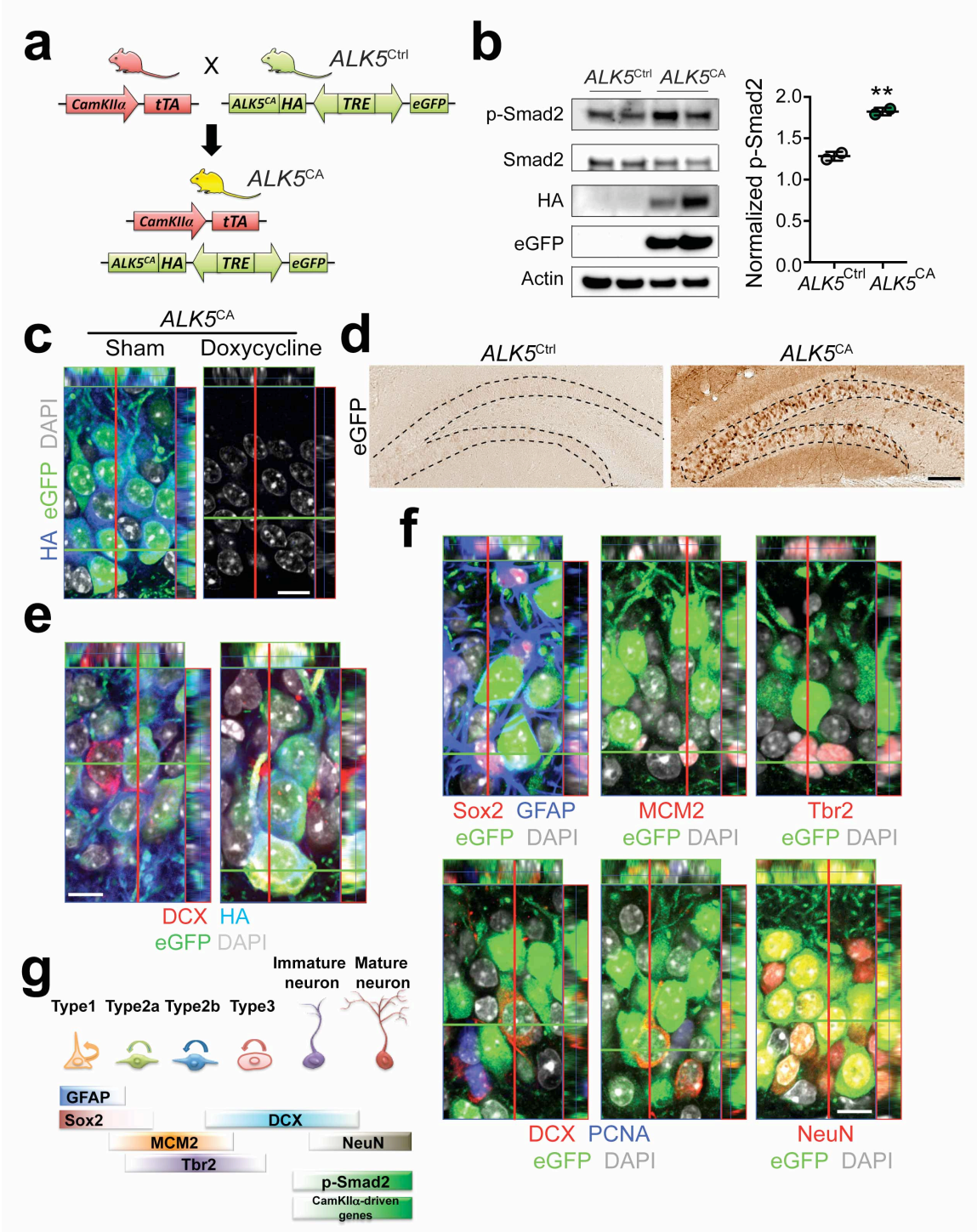

Supplementary Figure 6. Construction and characterization of *ALK5*^{CA} transgenic mice. (a) Diagram of gene constructs used to create *ALK5*^{CA} mice. (b) Immunoblots and quantification of p-Smad2 in hippocampal lysates from 3-month-old *ALK5*^{Ctrl} and *ALK5*^{CA} mice probed with antibodies against p-Smad2, Smad2, HA, eGFP, and actin. P-Smad2 signal intensity was normalized against Smad2. n = 2 mice per group. Full-length blots are presented in Supplementary Figure 10. Data are presented as mean + s.d. $^{**}P$ = 0.0085, Student's t-test. The experiments were independently performed twice. (c)

Representative orthogonal projections from confocal Z-stack images of the dentate gyrus of 4-month-old *ALK5*^{CA} mice before and after treatment with doxycycline immunostained for eGFP and HA. (d) eGFP expression in the dentate gyrus (dotted line) of *ALK5*^{CA} mice, but not of *ALK5*^{Ctrl} mice detected by immunohistochemistry. (e) Representative orthogonal projections from confocal Z-stack images of the dentate gyrus of 3-month-old *ALK5*^{CA} mice immunostained for eGFP, HA, and DCX. (f) Representative orthogonal projections from confocal Z-stack images of the dentate gyrus of 3-month-old *ALK5*^{CA} mice immunostained for eGFP in combination with Sox2 plus GFAP, MCM2, Tbr2, DCX plus PCNA, and NeuN. (g) Scheme depicting expression patterns of p-Smad2 and CamKIIα-driven genes during neuronal development based on characterization with specific neuronal development markers. DAPI stains nuclei. Scale bar is 100 µm in (d) and 10 µm in (c,e,f).

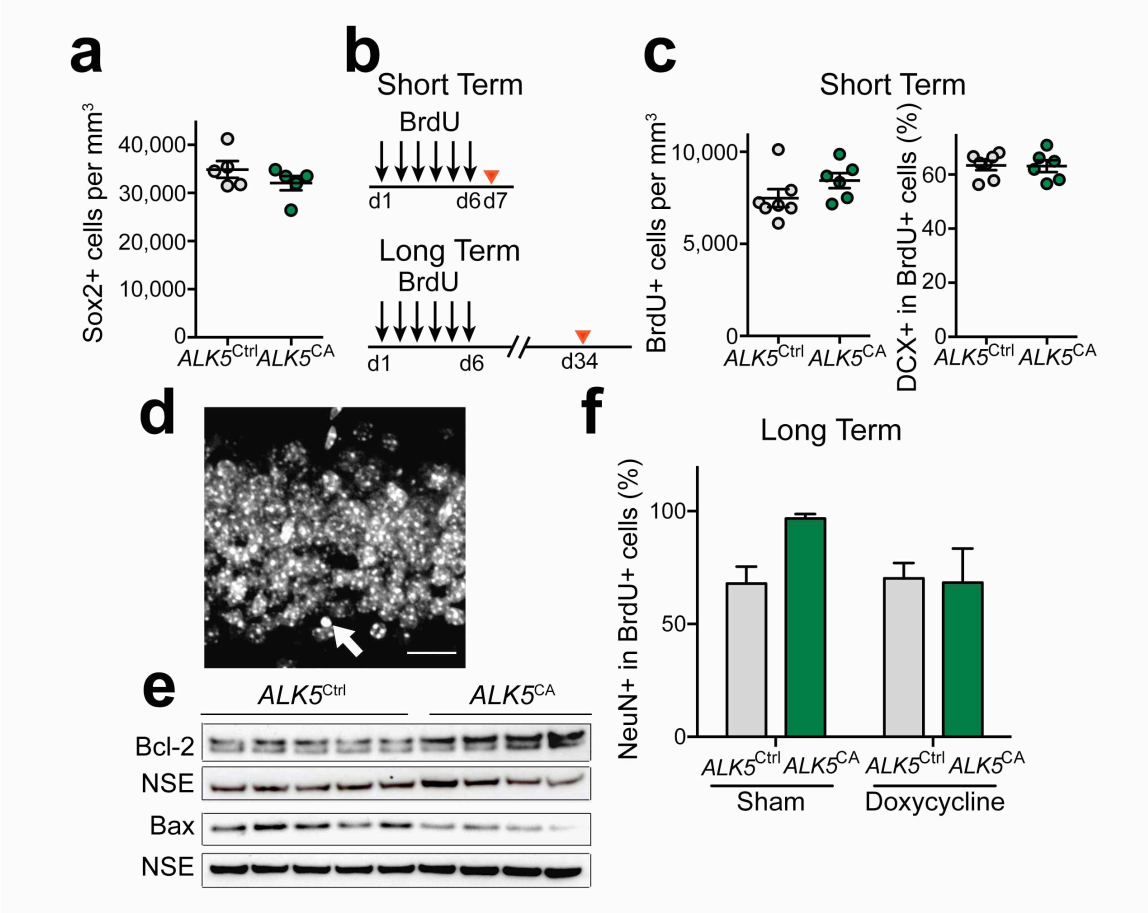

Supplementary Figure 7. Constitutive activation of ALK5 in forebrain neurons is not affecting neural stem cell pool and production of committed neurons, but is reducing apoptotic markers and increasing newborn neuron survival in the dentate gyrus. (a) Quantification of Sox2+ cells in the SGZ of the dentate gyrus of 3-month-old *ALK5*^{Ctrl} and *ALK5*^{CA} mice (n = 5 mice per group, 5 sections per mouse, $P = 0.2514$). (b) Experimental design for long-term and short-term BrdU-labeling paradigms. (c) Quantification of the total number of BrdU labeled cells and the percentage of BrdU and DCX double-labeled cells in the dentate gyrus of *ALK5*^{Ctrl} (n = 7) and *ALK5*^{CA} (n = 6) mice (3-month-old) 1 day after BrdU administration. Five sections per mouse. (d) A representative confocal image of DAPI staining in the dentate gyrus of 3-month-old *ALK5*^{CA} mice. Arrow points to an apoptotic cell with a pyknotic nucleus (condensed DAPI staining). Scale bar, 20 µm. (e) Immunoblots of hippocampal lysates from 3-month-old *ALK5*^{Ctrl} (n = 5) and *ALK5*^{CA} (n = 4) mice probed with antibodies against Bcl-2, Bax, and NSE. Full-length blots are presented in Supplementary Figure 10. (f) Quantification of BrdU and NeuN double-labeled newborn neurons in the dentate gyrus of 4-month-old *ALK5*^{Ctrl} and *ALK5*^{CA} mice 28 days after BrdU administration before and after doxycycline treatment (n = 4 mice per group, 5 sections per mouse). Doxycycline × genotype interaction $F(1,12) = 2.783$, $P = 0.1211$; doxycycline treatment $F(1,12) = 2.036$, $P = 0.1791$; genotype $F(1,12) = 2.134$, $P = 0.1697$; Data are presented as mean ± s.e.m. Student's t-test in (a,c). Two-way ANOVA in (f).

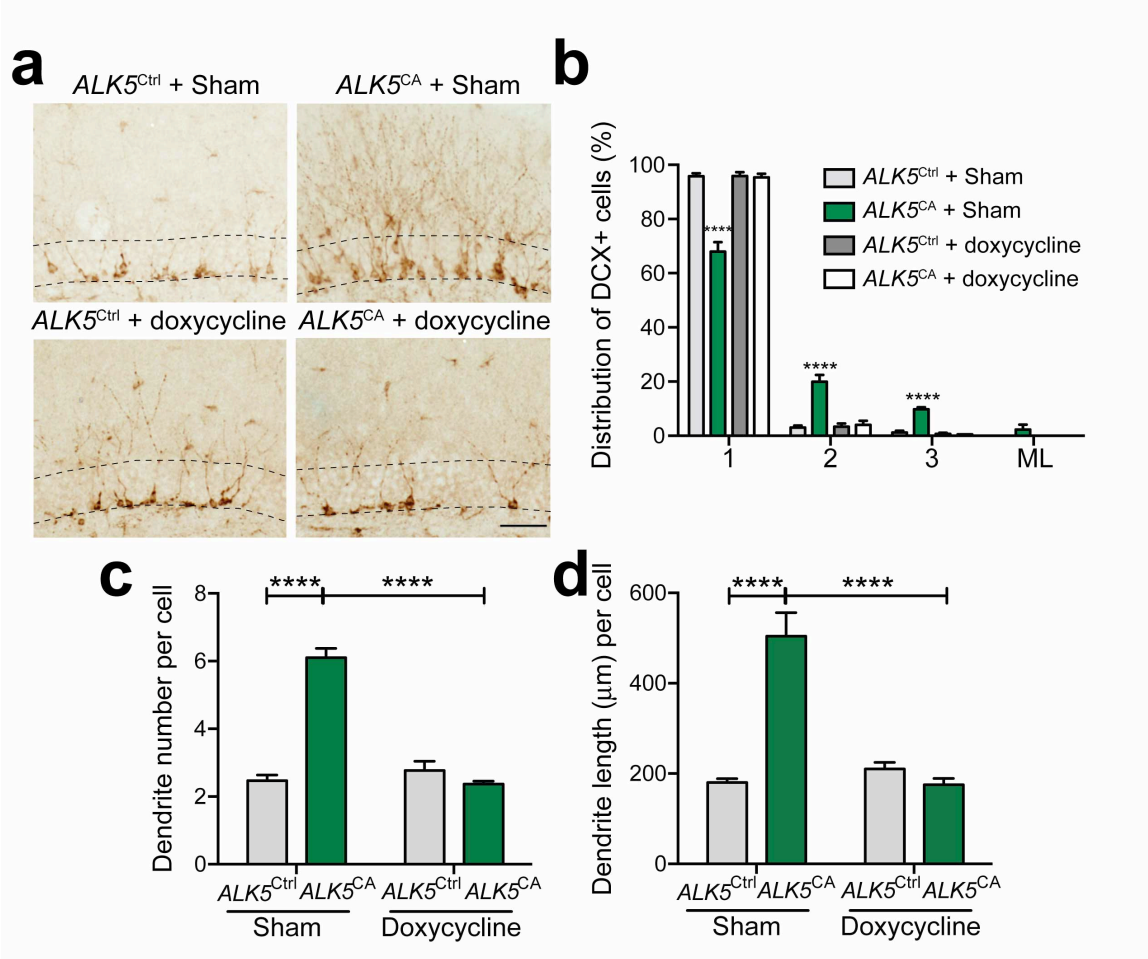

Supplementary Figure 8. Doxycycline treatment suppresses accelerated migration and dendritic development of newborn neurons in *ALK5*^{CA} mice. (a) Immunohistochemical detection of DCX labeled neurons in the dentate gyrus (dotted line) from 4-month-old *ALK5*^{Ctrl} and *ALK5*^{CA} mice before and after doxycyclline treatment. (b) Relative distribution of DCX labeled cells in *ALK5*^{Ctrl} and *ALK5*^{CA} mice before and after doxycycline treatment in the ML and three evenly separated layers of the dentate gyrus. (c,d) Dendritic development as quantified by dendritic number (c) and length (d) of DCX labeled cells from *ALK5*^{Ctrl} and *ALK5*^{CA} mice before and after doxycycline treatment. Scale bar, 50 µm. n = 4 mice per group. In (c), doxycycline × genotype interaction $F(1,12) = 59.12$, $P < 0.0001$; doxycycline treatment $F(1,12) = 42.25$, $P < 0.0001$; genotype $F(1,12) = 34.91$, $P < 0.0001$. In (d), doxycycline × genotype interaction $F(1,12) = 40.28$, $P < 0.0001$; doxycycline treatment $F(1,12) = 27.99$, $P = 0.0002$; genotype $F(1,12) = 26.15$, $P = 0.0003$. Data are presented as mean + s.e.m. ****$P < 0.0001$, one-way ANOVA, Tukey's post-hoc test (b); two-way ANOVA, Sidak's post-hoc test (c,d).

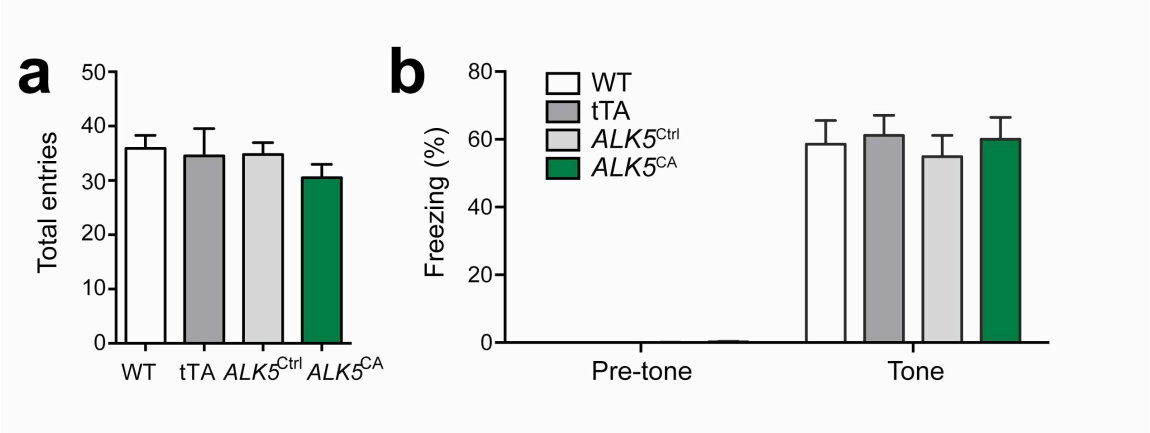

Supplementary Figure 9. *ALK5*^{CA} mice do not show any changes in total number of entries in the Y maze or the percentage of freezing under pre-tone and tone conditions in fear conditioning compared with genotype-matched control mice. (a) Total number of entries in the Y maze was measured from 3-month-old male WT, tTA, *ALK5*^{Ctrl}, and *ALK5*^{CA} mice. n = 18 mice per group. (b) Fear conditioning assessed by the percentage of freezing was displayed by 3-month-old male WT, tTA, *ALK5*^{Ctrl}, and *ALK5*^{CA} mice before tone and when re-exposed 24 hours later to the tone. n = 11 mice per group. In (b), time × genotype interaction $F(3,40) = 0.1782$, $P = 0.9106$; time $F(1,40) = 330.9$, $P < 0.0001$; genotype $F(3,40) = 0.1832$, $P = 0.9072$. One-way ANOVA, Tukey's post-hoc test (a); Two-way repeated-measures ANOVA, Bonferroni's post-hoc test (b).

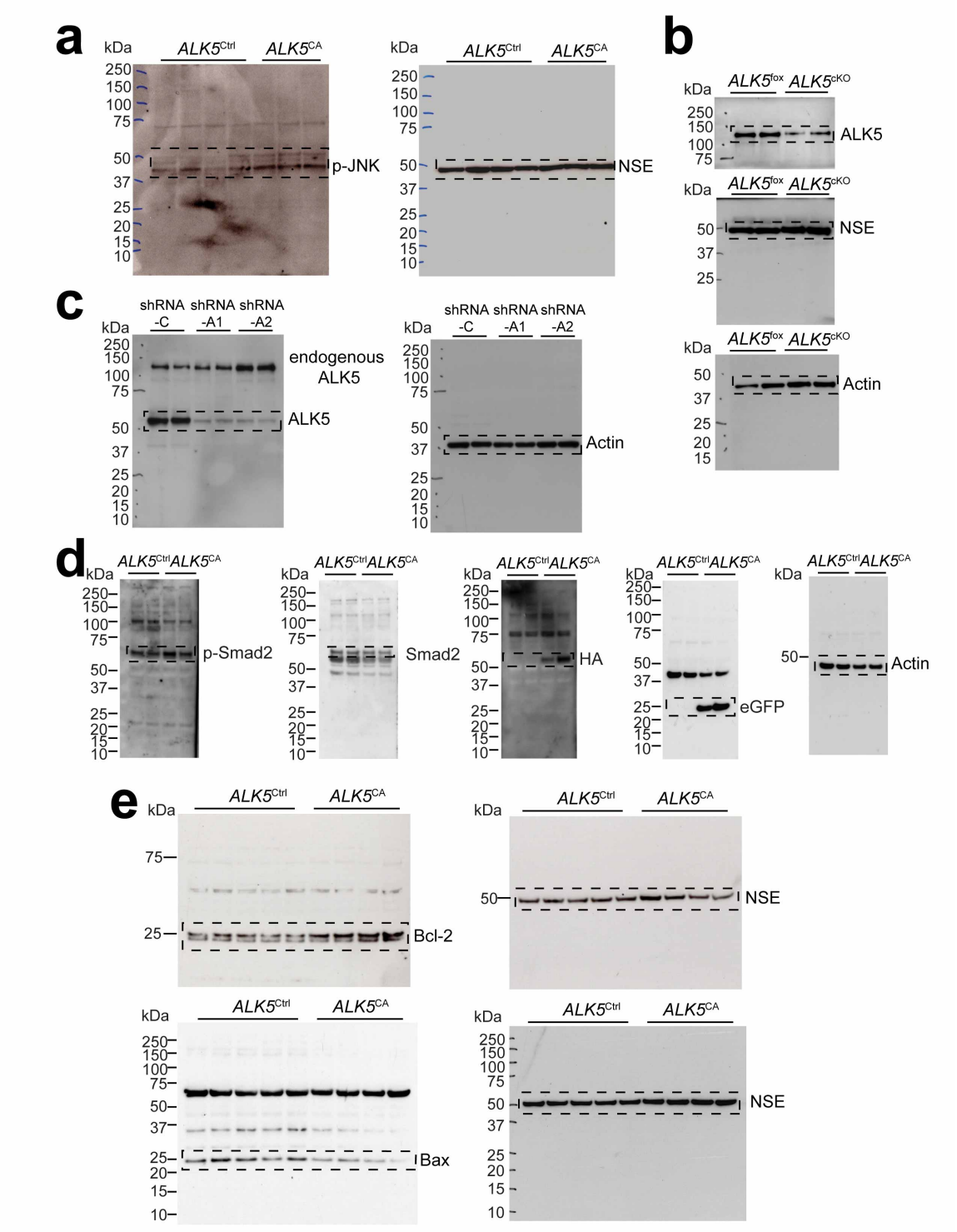

Supplementary Figure 10. Full-length blots presented in figures. The bands of interest are displayed within the dashed boxes. (a) Full-length blots of Figure 6c. (b) Full-length blots of Supplementary Figure 1b. (c) Full-length blots of Supplementary Figure 4b. (d) Full-length blots of Supplementary Figure 6b. (e) Full-length blots of Supplementary Figure 7e.

Supplementary Table 1. List of 28 differentially regulated genes in *ALK5*^{CA} compared with *ALK5*^{Ctrl} mice.

Symbol	Gene Name	Average Signal *ALK5*^{Ctrl}	Average Signal *ALK5*^{CA}	*P*-value	Function
Efcab3	EF-hand calcium binding domain 3	68.4723	11.3260	0.000023	Modulation of Ca(2+) signals
Doc2b	Double C2, beta	399.4887	156.4683	0.000311	Intracellular vesicle trafficking
Iqgap2	IQ motif containing GTPase activating protein 2	709.3116	473.0230	0.000601	Cell morphology and motility
Btg1	B-cell translocation gene 1	1314.2553	952.0877	0.001258	Cell growth and differentiation
Scg2	Secretogranin II	693.7335	409.4549	0.001979	Sorting of neuropeptides
Lypd1	Ly6/Plaur domain containing 1	616.1396	397.3760	0.002283	Possible tumor suppressor
Mbp	Myelin basic protein	788.6052	479.6385	0.003180	Formation of myelin membrane
Marcksl1	MARCKS-like 1	276.2271	191.3930	0.004089	Calmodulin signal transduction
Ccnd1	Cyclin D1	316.2127	189.4417	0.005014	Cell cycle
C1ql2	Complement component 1, q subcomponent-like 2	1080.3596	318.2034	0.006235	Developmental elimination of synapses
Grp	Gastrin releasing peptide	404.5876	203.2626	0.007653	Gastrin release
Prosapip1	ProSAPiP1 protein	1104.8557	759.7809	0.008055	Components of the postsynaptic density
Pdyn	Prodynorphin	157.7418	75.1392	0.009379	Apoptosis, response to pain
Spata13	Spermatogenesis associated 13	388.8699	192.9268	0.009719	Spermatogenesis
Dsp	Desmoplakin	61.5217	21.7805	0.018304	Cell junction
Kif1b	Kinesin family member 1B	135.7248	268.1401	0.000410	Neuronal migration, organelle transport
Car4	Carbonic anhydrase 4	644.9824	2000.4487	0.000590	Reversible hydration of carbon dioxide
Ppp1r13b	Protein phosphatase 1, regulatory (inhibitor) subunit 13B	130.4044	265.3408	0.000626	Apoptosis
Punc	Putative neuronal cell adhesion molecule	71.5303	226.9238	0.000626	Axon guidance
Kns2	Kinesin 2	289.9667	715.9435	0.002399	Neuronal migration, organelle transport
Ryr1	Ryanodine receptor 1	104.5700	178.1922	0.002787	Calcium release, neuronal differentiation
Tbr1	T-box brain gene 1	198.5189	560.9811	0.003986	Cortical laminar organization
Klc1	Kinesin light chain 1	2487.4947	4141.5760	0.004242	Neuronal migration, organelle transport
Megf9	Multiple EGF-like-domains 9	148.1874	301.5659	0.005945	Brain development
Gnal	Guanine nucleotide binding protein	45.7010	79.9383	0.009427	Transduction of neurotransmitters
Btbd6	BTB (POZ) domain containing 6	687.5807	879.9536	0.011363	Late neuronal development
C4a	Complement component 4A	105.0314	185.3765	0.021123	Activation of complement system
eGFP	Enhanced green fluorescent protein	14.9349	1906.9287	0.003753	Positive control